

Relation between copper L x-ray fluorescence and $2p$ x-ray photoelectron spectroscopies

Jun Kawai

Department of Metallurgy, Kyoto University, Sakyo-ku, Kyoto 606, Japan

Kuniko Maeda

The Institute of Physical and Chemical Research (RIKEN), 2-1 Hirosawa, Wako, Saitama 351-01, Japan

Katsumi Nakajima and Yohichi Gohshi

Department of Industrial Chemistry, University of Tokyo, 7-3-1 Hongo, Bunkyo-ku, Tokyo 113, Japan

(Received 13 April 1993)

$L\alpha_{1,2}, \beta_1(L_{3,2}-V)$ x-ray fluorescence spectra (XRF) and $2p_{1/2,3/2}$ x-ray photoelectron spectra (XPS) of various copper compounds are measured. It is found that the intensity of the high-energy hump of the Cu $L\alpha$ XRF has a correlation with that of the high-binding-energy satellite (corresponding to the poorly screened $2p^{-1}$ final state) of the Cu $2p_{3/2}$ XPS. While both the poorly screened peak in the $2p_{3/2}$ XPS and the high-energy hump in the $L\alpha$ XRF are strong for ionic divalent copper compounds, both of them are very weak for covalent divalent copper compounds, and they exist for neither monovalent nor metallic copper compounds. It was believed that the high-energy hump of the $L\alpha$ XRF originated from the electron transition between $L_3M_{4,5}-M_{4,5}^2$ multiple-hole states, where the $L_3M_{4,5}$ double-hole state was created by the $L_{1,2}L_3M_{4,5}$ Coster-Kronig transition prior to the x-ray transition. In this context, the $L\alpha$ line shape, except for the high-energy hump, was believed to represent the Cu $3d$ electron density of states (DOS). Our results, however, exclude the possibility of the multiple vacancy satellite $2p^53d^8 \rightarrow 3d^7$ for the origin of the high-energy hump of the $L\alpha$ XRF of the divalent copper compounds. It is concluded that the major portion of the high-energy hump of the $L\alpha$ XRF of the divalent copper compounds is due to the transition between the poorly screened states $2p^53d^9 \rightarrow 3d^8$. Consequently, it is also concluded that the $L\alpha$ line shape does not directly represent the $3d$ DOS but the high-energy hump hidden in the $L\alpha$ main line represents the $3d$ DOS. We also conclude that the $L\alpha$ main line originates from the charge-transfer effect.

I. INTRODUCTION

The $L\alpha_{1,2}, \beta_1(L_{3,2}-V)$ x-ray emission spectra (XES), or x-ray fluorescence spectra (XRF) of copper compounds result from a mixture of the $2p^{-1} \rightarrow 3d^{-1}$ and $2p^{-1} \rightarrow 4s^{-1}$ electric dipole transitions. Here, V denotes the valence hole state, and L_3 and L_2 denote the $2p_{3/2}^{-1}$ and $2p_{1/2}^{-1}$ hole states, respectively. Because the intensity of the $2p^{-1} \rightarrow 4s^{-1}$ transition is negligibly small compared with that of the $2p^{-1} \rightarrow 3d^{-1}$ transition,¹ the $L\alpha_{1,2}$ x-ray lines are the $L_3-M_{4,5}$ ($2p_{3/2}^{-1} \rightarrow 3d_{3/2,5/2}^{-1}$) x-ray lines and the $L\beta_1$ x-ray line is the L_2-M_4 ($2p_{1/2}^{-1} \rightarrow 3d_{3/2}^{-1}$) x-ray line for a copper atom. In what follows, we call these lines $L\alpha$ and $L\beta$. When treating a copper atom in solids, it was believed that the copper $L\alpha$ and $L\beta$ line shapes represented the local (Cu) and partial ($3d$) electron density of states (DOS) of the compounds as reviewed by Kurmaev, Nefedov, and Finkelstein.² This equivalence between $3d$ DOS and $L\alpha$ x-ray line shapes was based on the fact that the crossover transition term $2p^{-1} \rightarrow \phi_L^{-1}$ was negligibly small compared with the one center term $2p^{-1} \rightarrow 3d^{-1}$, where ϕ_L denotes one of the ligand valence orbitals. Note here that the $M_{4,5}$ spin-orbit splitting (~ 0.3 eV) (Ref. 3) is negligibly small compared with the molecular-orbital splittings which are usually ~ 5 eV. Thus, the two x-ray lines, L_3-M_4 and L_3-M_5 x-ray lines are treated as a single line.

Redinger *et al.*^{4,5} and Marksteiner *et al.*⁶ calculated the Cu $L\alpha$ x-ray emission line shapes of copper oxide superconductors on the assumption that the $L\alpha$ x-ray line shapes were equivalent to the Cu $3d$ DOS. After these calculations, the L x-ray line shapes were measured to study the $3d$ DOS of copper oxide superconductors by Mariot *et al.*^{7,8} and Barnole *et al.*⁹ However, Mariot *et al.*⁸ found that satisfactory agreement between highly precise calculations of the local-density-functional theory⁴⁻⁶ and the Cu $L\alpha$ experiment existed only for Cu_2O ; the experimental results for CuO and copper oxide superconductors did not agree with the calculations as shown in Fig. 1. Feldhütter, Šimůnek, and Wiech¹⁰ again found that the calculated $3d$ DOS (Refs. 4-6) did not agree with the measured Cu L x-ray line shape. Kaduwela *et al.*¹¹ measured and calculated the $L\alpha$ line shape of copper oxides; their *ab initio* calculations again failed to give a satisfactory agreement with the experimental spectra for divalent copper compounds. Since those calculations by Redinger *et al.*^{4,5} Marksteiner *et al.*⁶ and Kaduwela *et al.*¹¹ were very reliable, and also since their calculations gave very similar results, the disagreement between calculation and experiment indicates that the one-electron approximation^{12,13} is not valid for divalent copper compounds though it works very well for the calculations of the x-ray emission spectra of typical-element compounds such as B_6O ,¹⁴ C_{60} ,¹⁵ and C_{70} ,¹⁶ as well as monovalent copper compounds.

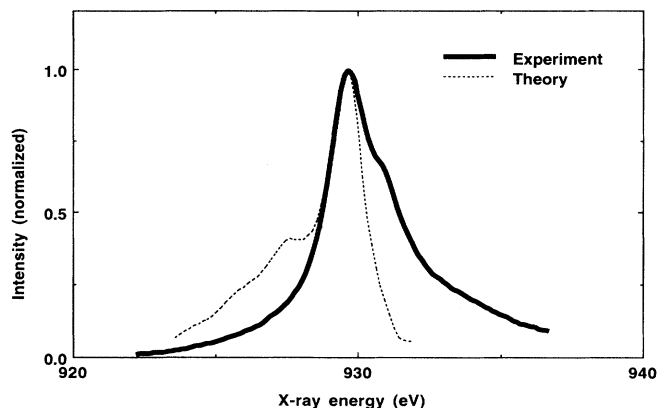


FIG. 1. Comparison between experiment [Barnole *et al.* (Ref. 9)] and theory [Redinger *et al.* (Ref. 4)] for copper oxide Cu $L\alpha$ line shapes.

Kawai and co-workers^{17,18} used the charge-transfer effect, which was one of the many-electron effects, to explain the narrow line shapes of the Cu $K\alpha_1$ ($1s^{-1} \rightarrow 2p_{3/2}^{-1}$) and Ni $K\beta$ ($1s^{-1} \rightarrow 3p^{-1}$) x-ray fluorescence spectra. This charge-transfer effect was originally introduced by van der Laan *et al.*¹⁹ and Zaanen, Sawatzky, and Allen²⁰ to interpret the satellite structure of transition-metal x-ray photoelectron spectra. The unoccupied $3d$ orbital in the charge-transfer-type transition-metal compounds²⁰ has a shallower binding energy than the ligand (e.g., oxygen) $2p$ orbital in the ground state as shown in Fig. 2. The $3d$ orbital energy becomes deeper than the ligand $2p$ orbital energy after the creation of the $2p^{-1}$ core hole (see Fig. 2). That is to say, when the $2p^{-1}$ core hole is created, the Cu $3d$ and the ligand $2p$ orbital cross each other,²¹ and at this moment, the $3d$ hole will be transferred from copper to the ligand $2p$ orbital in a finite probability as illustrated in Fig. 2. Tanaka, Okada, and Kotani,²²⁻²⁴ Hague *et al.*,^{25,26} and Kawai and co-workers^{3,27-30} suggested the importance of the charge-transfer effect for the interpretation of the $L\alpha$ x-ray emission line shapes of copper

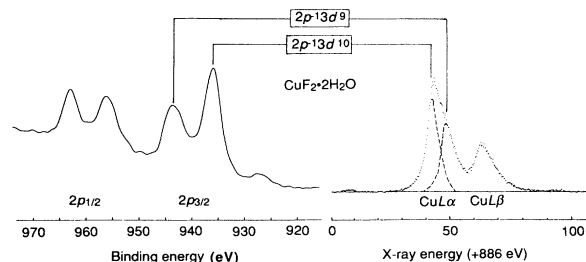


FIG. 3. Relation between Cu $2p$ XPS and Cu $L\alpha$ XRF proposed in Ref. 3. The spectra shown are measured XPS and XRF spectra of powder form $\text{CuF}_2 \cdot 2\text{H}_2\text{O}$.

oxides. The common feature of Refs. 3 and 22–30 is that they have pointed out that the $L\alpha$ main peak is not the $2p^5 3d^9 \rightarrow 3d^8$ transition but the $2p^5 3d^{10} \phi_L^{-1} \rightarrow 3d^9 \phi_L^{-1}$ transition for divalent copper compounds which have nominally $3d^9$ electron configuration in the ground state. Hague *et al.*²⁵ concluded that the poorly screened XES satellite ($2p^5 3d^9 \rightarrow 3d^8$), which corresponded to the XPS poorly screened final state, did not exist for x-ray emission spectra. However, Kawai and co-workers^{3,27-30} proposed that the high-energy hump in the $L\alpha$ XRF corresponded to the poorly screened XPS satellite as shown in Fig. 3, where the measured $\text{CuF}_2 \cdot 2\text{H}_2\text{O}$ XPS and XRF spectra are shown. The 5–10-eV high-energy hump of the $L\alpha$ XRF main line corresponds to the poorly screened peak (943 eV in binding energy) in XPS. The same correspondency also holds between $L\beta$ XRF and $2p_{1/2}$ XPS, though they are smeared by the possible $L_2 L_3 V$ Coster-Kronig transition. Kawai and Maeda,^{3,27} calculated the $L\alpha$ multiplet structure, which was the mixture of the $2p^5 3d^{10} \phi_L^{-1} \rightarrow 3d^9 \phi_L^{-1}$ and the $2p^5 3d^9 \rightarrow 3d^8$ transitions, using the LS coupling scheme of atoms. These calculations resulted in a satisfactory agreement between theory and experiment for divalent copper compounds. This $L\alpha$ high-energy hump has long been regarded as a multiple ionization satellite ($2p^5 3d^{-1} \rightarrow 3d^{-2}$) due to the $L_{1,2} L_3 M_{4,5}$ Coster-Kronig transition as shown in Fig. 4, as was described by

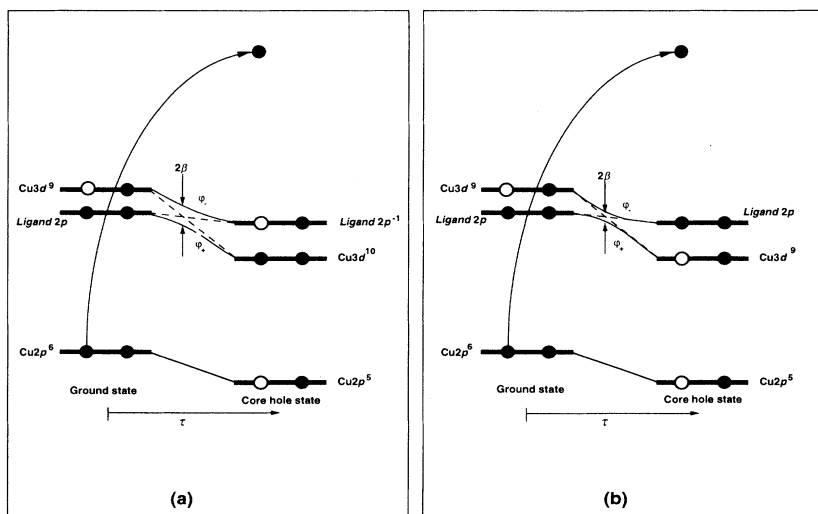


FIG. 2. Schematic illustration of the charge-transfer effect for the late-transition-metal compounds at the creation of the $2p^{-1}$ core hole. (a) Large $|\beta|$ case, and (b) small $|\beta|$ case.

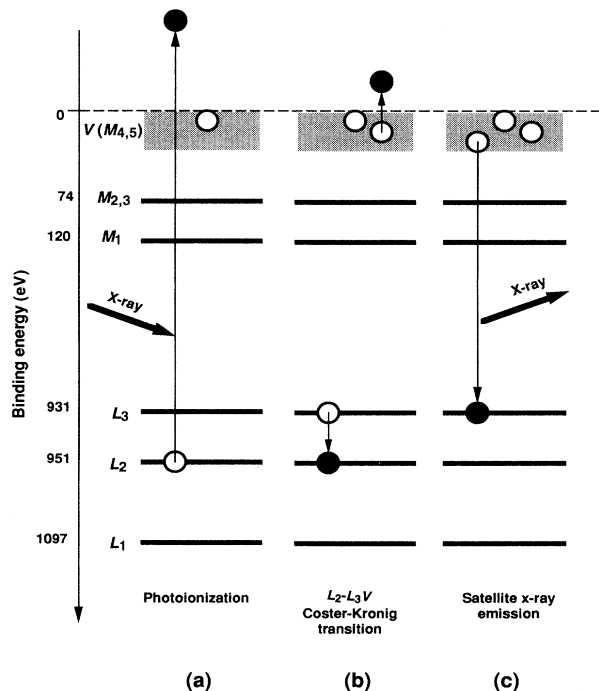


FIG. 4. Schematic illustration of the origin of the $L\alpha$ multivacancy satellite. L_2L_3V Coster-Kronig transition prior to the $L\alpha$ x-ray emission was believed to cause the $2p^53d^8 \rightarrow 3d^7$ satellite emission (high-energy hump of the Cu $L\alpha$ line). The diagram line was believed to be the $2p^53d^9 \rightarrow 3d^8$ transition (Cu $L\alpha$ main peak).

Wassdahl *et al.*³¹ In the present paper, however, the portion of the Coster-Kronig satellite is negligibly small for the origin of the high-energy hump as will be discussed below.

Galakhov and co-workers^{32–34} and Butorin *et al.*^{35,36} measured the Cu $L\alpha$ spectra of copper oxide superconductors to study the energy of the Cu $3d$ DOS maximum on the basis that the $L\alpha$ spectra represented the Cu $3d$ DOS. It was true that these papers^{32–36} correctly assigned that the Cu $L\alpha$ was the $2p^53d^{10}\phi_L^{-1} \rightarrow 3d^9\phi_L^{-1}$ transition but, since they erroneously regarded that the $L\alpha$ main-peak energy equaled to the energy of the $3d$ DOS maximum in the ground state, they erroneously concluded that the O $2p$ orbital energy was shallower than the Cu $3d$ orbital energy for copper oxide superconductors. This was true for core-hole state, but not for the ground state of the copper oxides. This conclusion had a contradiction to the generally accepted energy-level ordering shown in Fig. 2; Cu $3d$ is shallower than O $2p$ in the ground state. Because the charge-transfer effect is important for late-transition-metal compounds as proposed by Zaanen, Sawatzky, and Allen,²⁰ the energy of the $3d$ DOS maximum interpreted in Refs. 32–36 was not correct. The observed $3d$ DOS maximum was shifted by the charge-transfer energy from the ground-state $3d$ DOS maximum.

It should be noted that the interpretations of the $L\alpha$ spectra of metallic copper in the literature^{37,38} do not need to be changed. This is because the charge transfer

due to the presence of the $2p^{-1}$ core hole is only possible through the $4s$ level since the $3d$ level of metals is already filled by electrons. The satisfactory agreement between theory and experiment for Cu_2O described above⁸ can also be explained by the absence of the charge-transfer effect, because Cu_2O has nominally $3d^{10}$ electron configuration; thus, the charge-transfer effect is not important.

We report in the present paper the measurements of both the $L\alpha$ XRF and $2p_{3/2}$ XPS of various copper compounds to prove the relation illustrated in Fig. 3, which was only a theoretical prediction in the previous paper.³

II. EXPERIMENT

Some of the measured samples were commercially available compounds: Cu(metal), CuSO_4 , CuF_2 , CuCl_2 , CuO, copper(II) phthalocyanine [Cu(Pc)], copper(II) acetylacetonate [$\text{Cu}(\text{acac})_2$], CuI, CuBr, CuCl, and Cu_2O . Other superconductor related compounds were prepared by the present authors by the method in the literature.^{39–41} Y-Ba-Cu-O (YBCO), La-Sr-Cu-O (LSCO), and Bi-Sr-Ca-Cu-O (BSCCO). The prepared samples were checked by the powder x-ray-diffraction method. Though the YBCO was not a superconducting phase but the tetragonal phase, the x-ray spectra were expected to be similar to the superconducting phase.⁴²

The XRF spectra were measured with a Bragg type (flat analyzing crystal) x-ray fluorescence spectrometer, RIGAKU 3070. An end-window Rh-anode x-ray tube was used for primary excitation with 50 kV and 50 mA. The analyzing crystal was TAP(100) ($2d = 25.76 \text{ \AA}$). A gas-flow proportional counter was used to detect the x rays. The 2θ scan range was from 58° to 66° by 0.02° step. The dwell time for one channel was 5 s. Since the third-order Bragg reflection of the Rh $L\alpha$ line emerged at 35 eV below the Cu $L\alpha$ line (very small peak at $\sim 895 \text{ eV}$ in Figs. 3 and 5), a single-channel analyzer was used to avoid counting the Rh signal.

The XPS spectra were measured by a VG ESCA-LAB MKII spectrometer with Al or Mg anode tube. The dual anodes were used to discriminate unknown Auger peaks. Powder samples were set to the sample holder by double-sided 3M adhesive tape. The ceramics samples were filed in a vacuum using an alumina stick held by a holder reported by Jayne.⁴³ The spectra were smoothed by the Savitzky-Golay method⁴⁴ with 5 points and 10 iterations and then subtracted the background by the method of Shirley.⁴⁵ Then, the intensity of the satellite (poorly screened final state) relative to that of the main line (well-screened final state) was determined by numerically integrating the intensities of these lines.

III. RESULTS AND DISCUSSION

The representative $L\alpha, \beta$ spectra of Cu_2O and CuO are shown in Fig. 5. It is found from Fig. 5 that a hump exists at a 5–10-eV high-energy shoulder of the $L\alpha$ line of CuO, but that it does not exist in a Cu_2O spectrum. This is a common difference between divalent and monovalent

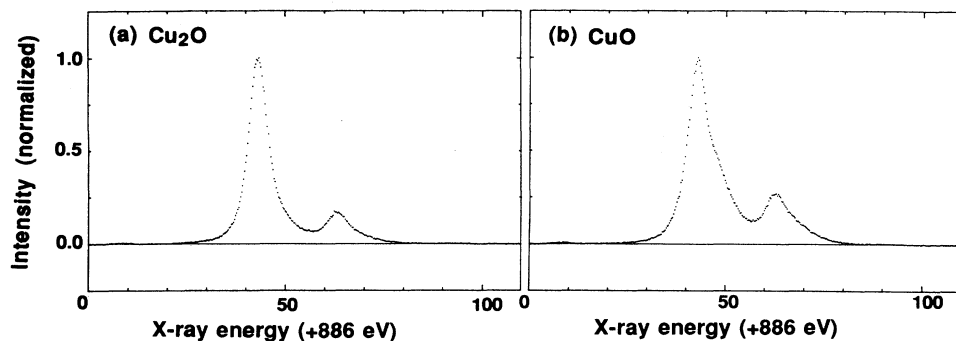


FIG. 5. Cu $L_{\alpha,\beta}$ x-ray fluorescence spectra of (a) Cu_2O and (b) CuO .

copper compounds, e.g., CuCl_2 and CuCl , and CuBr_2 and CuBr .

We introduce a parameter, which is an $L\alpha$ linewidth, to estimate the high-energy hump intensity conveniently; we have assumed that the full width at $\frac{1}{3}$ maximum ($\text{FW}_{\frac{1}{3}\text{M}}$) of the peak is a good index of describing the high-energy hump intensity. This is because the low-energy side of the $L\alpha$ line has a similar line shape among the copper compounds. We have plotted the $\text{FW}_{\frac{1}{3}\text{M}}$ against the satellite intensity of the $2p_{3/2}$ XPS spectra as shown in Fig. 6. It is found from Fig. 6 that the $L\alpha$ line width is large when the $2p$ XPS satellite is strong and it is small when the XPS satellite is weak. This rule holds not only for divalent copper compounds but also for metallic and monovalent copper compounds which have no XPS satellite. The only exception is $\text{Cu}(\text{acac})_2$, which has two satellites due to a large overlap between two kinds of ligands (C and O).⁴⁶ Therefore, those compounds which have one or fewer than one XPS satellite have a good correlation between the Cu $2p$ XPS satellite intensity and the XRF high-energy hump intensity; if the $L\alpha$ XRF high-energy hump intensity is strong, then the poorly screened $2p$ XPS satellite is also strong; if the former is weak, then the latter is also weak.

Consequently, the XRF line shape has similar information on the electronic structure of the copper compounds to the XPS line shape. It is true that the XPS spectra are obtainable with much higher resolution than the XRF spectra. However, the XPS spectra are very sensitive to the surface contamination, thus it is very difficult to measure the CuF_2 XPS spectrum in the powder form, because the CuF_2 powder is easily hydrated. The $L\alpha$ XRF can discriminate CuF_2 from $\text{CuF}_2 \cdot 2\text{H}_2\text{O}$ as shown in Fig. 7. Therefore the XRF is useful for measuring the poorly screened portion of very unstable compounds that are problematic with XPS measurements.

It had long been believed that the high-energy hump was a multiple-ionization satellite created by the $L_{1,2}L_3M_{4,5}$ Coster-Kronig transitions [see Fig. 4(b)] prior to the $L_3-M_{4,5}$ x-ray transitions. On this basis, the high-energy hump in the $L\alpha$ x-ray spectra was believed to originate from the $L_3M_{4,5}-M_{4,5}^2$ x-ray transitions (multiple-hole satellite; one of the $M_{4,5}$ holes is a spectator hole) as shown in Fig. 4(c). Therefore, the x-ray ener-

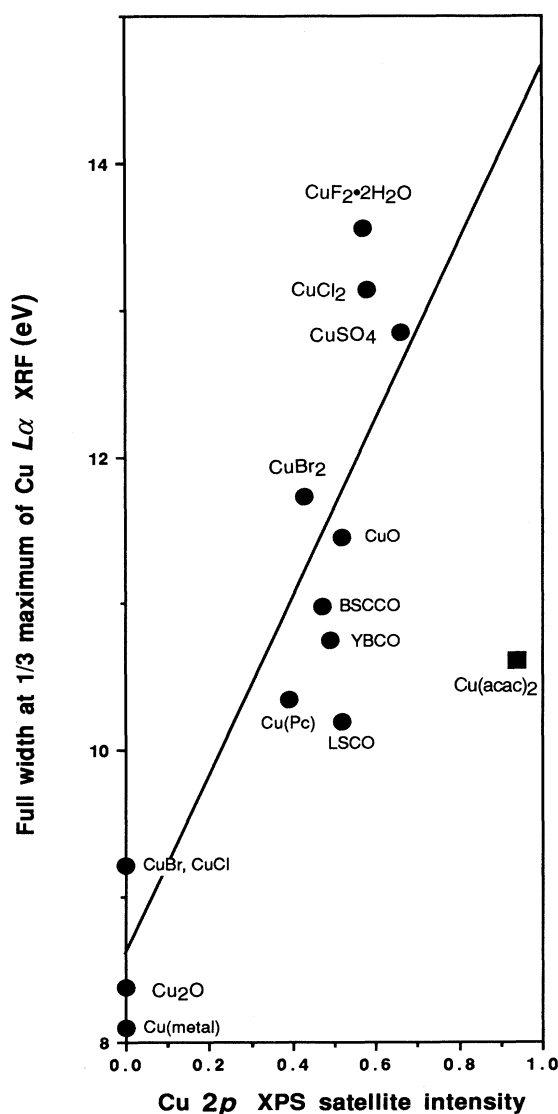


FIG. 6. Relation between the Cu $2p$ XPS satellite intensity (relative to the $2p$ main line) and the full width at $\frac{1}{3}$ maximum ($\text{FW}_{\frac{1}{3}\text{M}}$) of the $L\alpha$ XRF for various copper compounds. The solid line is the least-squares fit to data as denoted by the solid circles.

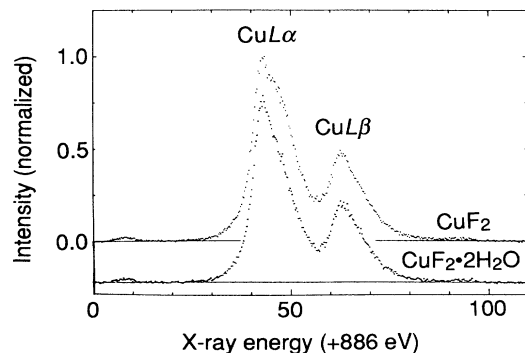


FIG. 7. L x-ray fluorescence spectra of CuF_2 and $\text{CuF}_2 \cdot 2\text{H}_2\text{O}$.

gy was believed to be shifted due to the presence of the spectator M hole. We believe that it is very difficult for the spectator hole to stay at the Cu site before and during the x-ray transition. This is because the $3d$ hole, which originates either from the Coster-Kronig transition or shake-off process⁴⁷ or which exists from the initial ground state because the compound is one of the divalent copper compounds, in the charge-transfer compounds is easily filled by one of the ligand electrons when the copper core hole is created. The ligand electrons are attracted by the core hole potential of the copper atom and the valence hole is quite easily transferred for the charge-transfer compounds since the transfer-matrix element ($|\beta|$, described below) is large for charge-transfer compounds. Since the shake-off probability of the charge-transfer compounds is very low because the charge-transfer compounds are covalent compounds,⁴⁸ it is enough to consider the Coster-Kronig process as the origin of the double-hole creation process.

If the high-energy satellite originates from the multiple-hole initial state ($L_3M_{4,5}$), which is created by the $L_{1,2}L_3M_{4,5}$ Coster-Kronig transition, then the high-energy hump becomes stronger when the $L\beta$ (L_2-M_4) intensity becomes weaker. This is because for those compounds of strong $L_{1,2}L_3M_{4,5}$ Coster-Kronig transitions, the decay rate of the L_2 hole by the $L\beta$ x-ray emission becomes smaller than the compounds of weak $L_{1,2}L_3M_{4,5}$ Coster-Kronig transitions. We have plotted the relation between the $L\alpha$ hump intensity ($\text{FW}_{\frac{1}{3}}M$) and the Coster-Kronig transition rate ($L\beta/L\alpha$ ratio) in Fig. 8 to study the origin of the high-energy hump of the $L\alpha$ XRF whether it originates from the multiple-hole $L_3M_{4,5}$ satellite or charge-transfer effect (Fig. 3). If the $L\alpha$ hump originates from multiple-hole satellite due to the Coster-Kronig transition prior to the $L\alpha$ x-ray emission, then the data in Fig. 8 tend to lie on line A and B in Fig. 8. However, the experimental tendency is, in fact, inverse to this; the experimental data lie between lines C and D and E and F in Fig. 8. For example, if one studies the $\text{Cu } L\alpha$ of CuF_2 or $\text{CuF}_2 \cdot 2\text{H}_2\text{O}$, then the $L\beta/L\alpha$ intensity ratio is more than 0.4, but the satellite is also very strong, as is found from Fig. 7. On the other hand, the metallic copper has weak $L\beta/L\alpha$ intensity ratio even in the self-absorption free spectrum⁴⁹ as is shown in Fig. 8, and in

spite of this, the high-energy hump is weak. These facts provide us an evidence that the high-energy hump is not due to the Coster-Kronig transition but due to the charge-transfer effect of Fig. 3.

To discuss the degree of charge transfer at the moment of the level crossing, we have assumed in Fig. 2 the two-atom molecule Cu ligand; it is easy to extend this to a cluster such as CuO_4 by introducing molecular orbitals expressed by a linear combination of atomic orbitals. The molecular orbitals φ_+ (deeper level) and φ_- (shallower level) at the level crossing in Fig. 2 can be expressed as

$$\begin{aligned}\varphi_+ &= \frac{1}{\sqrt{2(1+S)}}(\chi_A + \chi_B), \\ \varphi_- &= \frac{1}{\sqrt{2(1-S)}}(\chi_A - \chi_B),\end{aligned}\quad (1)$$

where $\chi_A = |\text{Cu } 3d\rangle$ and $\chi_B = |\phi_L\rangle$, and $S = \langle \chi_A | \chi_B \rangle$. The effective one-electron Hamiltonian is

$$\hat{h} = -\frac{1}{2}\Delta + V_{\text{Cu}}(r) + V_L(r), \quad (2)$$

where V_{Cu} and V_L are the copper and the ligand atomic potentials, respectively, and accidentally the degeneration occurs at the crossing point

$$\langle \chi_A | \hat{h} | \chi_A \rangle = \langle \chi_B | \hat{h} | \chi_B \rangle = \alpha. \quad (3)$$

If setting $\beta = \langle \chi_A | \hat{h} | \chi_B \rangle$, which is the transfer-matrix element described above, then we obtain the molecular-orbital eigenvalues of the effective one-electron Hamil-

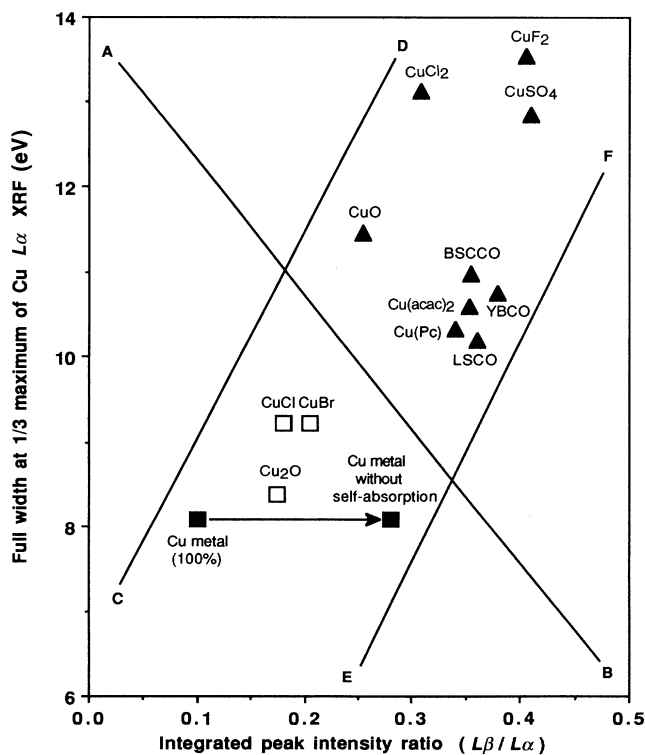


FIG. 8. Plot of the XRF high-energy hump intensity against the $L\beta/L\alpha$ integrated peak intensity ratio.

tonian in Eq. (2) as

$$\begin{aligned}\varepsilon_+ &= (\alpha + \beta)/(1 + S), \\ \varepsilon_- &= (\alpha - \beta)/(1 - S).\end{aligned}\quad (4)$$

Therefore, the energy separation in the avoided crossing is $\varepsilon_- - \varepsilon_+ = -2\beta$, because $S^2 \ll 1$ for copper compounds. Equation (3) is possible when the levels of Cu $3d$ and the ligand $2p$ are crossing each other. The two levels can cross because of the continuous change of V_{Cu} in Eq. (2) when the $2p$ photoelectron leaves. The Coulomb potential from the Cu $2p$ hole which is created by photoionization is gradually larger and larger when the photoelectron gradually leaves from the Cu atom. If the transfer-matrix element $|\beta|$ is large, then the Cu $3d$ hole is transferred from copper to the ligand site. However, when $|\beta|$ is small, the molecular orbitals almost cross each other, and the Cu $3d$ hole still remains in the $3d$ orbital after the crossing. This approximation holds when the photoionization event is sudden,⁴⁷ i.e., τ in Fig. 3 is much smaller than the classical electron circulation period in the $3d$ orbital. On the contrary, if τ is large enough, then the Cu $3d$ hole is adiabatically transferred to the ligand $2p$ orbital even when the transfer-matrix element $|\beta|$ is small. These situations are quite similar to the avoided crossing in the chemical reaction, where the electron transfer probability depends on the slope of the energy curve and the velocity with which a system crosses.⁵⁰⁻⁵³

Wassdahl *et al.*³¹ measured Cu $L\alpha$ x-ray spectra with and without the adiabatic condition. However, such an adiabatic measurement has many problems in it. Since the photoelectron kinetic energy of the threshold experiment of Wassdahl *et al.*³¹ was quite close to zero, the experimental condition was in the adiabatic limit, thus the charge-transfer probability is quite low. Therefore, in the threshold excitation, whether the atomic shake up is possible or not is one of the problems and whether the shake up in the molecular-orbital picture, i.e., nonadiabatic electron transfer from the ligand to the central metal ion, is possible or not is also an important problem. Therefore, the experiment of Wassdahl *et al.*³¹ could not discriminate the atomic process (M -shell vacancy) from the solid-state process (charge-transfer process from the neighbor atom).

The high-energy hump in Cu $L\alpha$ XRF is 3–5 eV higher than the Cu $L\alpha$ main peak. Though Kurmaev's group concluded that Cu $3d < O 2p$ on the assumption that the $L\alpha$ main peak equaled to the DOS maximum, we conclude that Cu $3d > O 2p$ provided that the $L\alpha$ high-energy hump represents the ground-state DOS, which agrees with the generally accepted level ordering, Cu $3d > O 2p$.

IV. CONCLUSIONS

We have measured both Cu $L\alpha$ x-ray fluorescence and Cu $2p$ x-ray photoelectron spectra of many copper compounds, metal, and alloys, and found that the Cu(II) compounds have a high-energy hump on the $L\alpha$ and $L\beta$ x-ray lines, and the Cu(I) compounds, metal, and alloys do not have the high-energy hump.

It has also been found that the intensity of the high-energy hump of the $L\alpha$ line correlates to the intensity of the high-energy satellite of the $2p_{3/2}$ XPS spectra. When the intensity of the $2p_{3/2}$ XPS satellite is strong [this is the case for ionic Cu(II) compounds such as CuF_2 , CuO , $CuCl_2$, etc.], then the high-energy hump of the $L\alpha$ x-ray fluorescence (emission) spectra is also strong. Contrary to this, when the $2p_{3/2}$ XPS satellite is weak [this is the case for covalent Cu(II) compounds such as high- T_c superconductors and phthalocyanine (Cu-N bond)], or the satellite is not at all present [this is the case for Cu(I) compounds, metal, or alloys], then the high-energy hump is also weak or does not exist at all in the x-ray emission spectra.

Usually, the transition-metal L x-ray emission spectral line shapes were regarded as being representative of the $3d$ local and partial electron density of state (DOS) in the compounds or alloys. However, we have shown that the $L\alpha$ high-energy hump shape corresponds to the $3d$ DOS for divalent copper compounds. The comparison between Ni $2p$ XPS and Ll, η XES by Wood and Urch⁵⁴ supports the validity of this conclusion for nickel compounds. As the XPS spectra consist of well-screened and poorly screened states, the x-ray emission spectra also have information on the well-screened and poorly screened states. Though we have neglected the possibility of the multiple hole as the origin of the $L\alpha$ high-energy hump, this is very small but not completely zero.^{55,56}

The linewidth of Cu $L\alpha$ of Cu(II) compounds is wider for ionic compounds than that for covalent compounds, Cu(I) compounds, metal, or alloys. Consequently, we conclude that the $L\alpha$ XRF line shape has similar information to the $2p_{3/2}$ XPS on the electronic structure of compounds or alloys.

ACKNOWLEDGMENTS

We thank Aiko Nakao (RIKEN) for her technical contribution to the XPS measurement, and the Division of Research Instruments Development, RIKEN, for making the alumina stick holder. Dr. R. Baba (Univ. of Tokyo) is greatly acknowledged for providing us a chance to use the RIGAKU x-ray fluorescence spectrometer.

¹J. H. Scofield, Phys. Rev. **179**, 9 (1969).

²E. Z. Kurmaev, V. I. Nefedov, and L. D. Finkelstein, Int. J. Mod. Phys. B **2**, 393 (1988).

³J. Kawai and K. Maeda, Spectrochim. Acta **46B**, 1243 (1991).

⁴J. Redinger, J. Yu, A. J. Freeman, and P. Weinberger, Phys. Lett. A **124**, 463 (1987).

⁵J. Redinger, A. J. Freeman, J. Yu, and S. Massidda, Phys. Lett. A **124**, 469 (1987).

⁶P. Marksteiner, J. Yu, S. Massidda, and A. J. Freeman, Phys. Rev. B **39**, 2894 (1989).

⁷J.-M. Mariot, V. Barnole, C. F. Hague, V. Geiser, and H.-J. Güntherodt, Solid State Commun. **64**, 1203 (1987).

- ⁸J.-M. Mariot, V. Barnole, C. F. Hague, G. Vetter, and F. Queyroux, *Z. Phys. B* **75**, 1 (1989).
- ⁹V. Barnole, J.-M. Mariot, C. F. Hague, C. Michel, and B. Raveau, *Phys. Rev. B* **41**, 4262 (1990).
- ¹⁰H.-O. Feldhütter, A. Šimůnek, and G. Wiech, *Solid State Commun.* **79**, 977 (1991).
- ¹¹A. P. Kaduwela, J. D. Head, W. K. Kuhn, and G. Andermann, *J. Electron Spectrosc. Relat. Phenom.* **49**, 183 (1989).
- ¹²D. S. Urch, *J. Phys. C* **3**, 1275 (1970).
- ¹³R. Manne, *J. Chem. Phys.* **52**, 5733 (1970).
- ¹⁴J. Kawai, K. Maeda, I. Higashi, M. Takami, Y. Hayasi, M. Uda, *Phys. Rev. B* **42**, 5693 (1990).
- ¹⁵J. Kawai, K. Maeda, M. Takami, Y. Muramatsu, T. Hayashi, M. Motoyama, and Y. Saito, *J. Chem. Phys.* **98**, 3650 (1993).
- ¹⁶J. Kawai and M. Motoyama, *Phys. Rev. B* **47**, 12 988 (1993).
- ¹⁷J. Kawai, Y. Nihei, M. Fujinami, Y. Higashi, S. Fukushima, and Y. Gohshi, *Solid State Commun.* **70**, 567 (1989).
- ¹⁸J. Kawai, M. Takami, and C. Satoko, *Phys. Rev. Lett.* **65**, 2193 (1990).
- ¹⁹G. van der Laan, C. Westra, C. Haas, and G. A. Sawatzky, *Phys. Rev. B* **23**, 4369 (1981).
- ²⁰J. Zaanen, G. A. Sawatzky, and J. W. Allen, *Phys. Rev. Lett.* **55**, 418 (1985).
- ²¹J. Kawai, *Nucl. Instrum. Methods Phys. Res. B* **75**, 3 (1993).
- ²²S. Tanaka, K. Okada, and A. Kotani, *J. Phys. Soc. Jpn.* **58**, 813 (1989).
- ²³S. Tanaka, K. Okada, and A. Kotani, *J. Phys. Soc. Jpn.* **60**, 3893 (1991).
- ²⁴S. Tanaka, K. Okada, and A. Kotani, *Physica C* **185-189**, 1489 (1991).
- ²⁵C. F. Hague, V. Barnole, J.-M. Mariot, and M. Ohno, *Phys. Scripta* **41**, 924 (1990).
- ²⁶C. F. Hague, J.-M. Mariot, V. Barnole, and C. Michel, *Physica C* **185-189**, 711 (1991).
- ²⁷J. Kawai and K. Maeda, *Physica C* **185-189**, 981 (1991).
- ²⁸K. Nakajima, J. Kawai, and Y. Gohshi, *Physica C* **185-189**, 983 (1991).
- ²⁹J. Kawai and K. Maeda, *RIKEN Accel. Prog. Rep.* **25**, 147 (1991).
- ³⁰J. Kawai, K. Nakajima, K. Maeda, and Y. Gohshi, *Adv. X-Ray Anal.* **35**, 1107 (1992).
- ³¹N. Wassdahl, J.-E. Rubensson, G. Bray, P. Glans, P. Bleckert, R. Nyholm, S. Cramm, N. Mårtensson, and J. Nordgren, *Phys. Rev. Lett.* **64**, 2807 (1990).
- ³²V. R. Galakhov, N. N. Yefremova, E. Z. Kurmayev, A. V. Postnikov, V. M. Cherkashenko, L. D. Finkel'shteyn, Yu. M. Yarmoshenko, and V. L. Kozhevnikov, *Phys. Met. Metall.* **64**, 197 (1987).
- ³³V. R. Galakhov, S. M. Butorin, L. D. Finkelstein, E. Z. Kurmayev, Yu. M. Yarmoshenko, V. A. Trofimova, and V. L. Kozhevnikov, *Physica C* **160**, 267 (1989).
- ³⁴V. R. Galakhov, S. M. Butorin, E. Z. Kurmaev, and M. A. Korotin, *Physica B* **168**, 163 (1991).
- ³⁵S. M. Butorin, V. R. Galakhov, L. D. Finkelstein, E. Z. Kurmaev, Yu. A. Teterin, M. I. Sosulnikov, S. M. Cheshnitsky, S. A. Lebedev, and A. I. Akimov, *Physica C* **177**, 8 (1991).
- ³⁶S. M. Butorin, V. R. Galakhov, E. Z. Kurmaev, Yu. B. Poltoratskii, and S. P. Tolochko, *Solid State Commun.* **84**, 995 (1992).
- ³⁷P. J. Durham, D. Ghaleb, B. L. Györfy, C. F. Hague, J.-M. Mariot, G. M. Stocks, and W. M. Temmerman, *J. Phys. F* **9**, 1719 (1979).
- ³⁸E. Z. Kurmaev, V. R. Galakhov, and A. V. Postnikov, *J. Phys. F* **15**, 2041 (1985).
- ³⁹R. J. Cava, R. B. van Dover, B. Batlogg, and E. A. Rietman, *Phys. Rev. Lett.* **58**, 408 (1987).
- ⁴⁰T. Hashemi, F. Golestani-Fard, Z. T. Al-Dhhan, and C. A. Hogarth, *Spectrochim. Acta* **43B**, 951 (1988).
- ⁴¹A. E. Bocquet, J. F. Dobson, P. C. Healy, S. Myhra, and J. G. Thompson, *Phys. Status Solidi B* **152**, 519 (1989).
- ⁴²M. Fujinami, H. Hamada, Y. Hashiguchi, and T. Ohtsubo, *Jpn. J. Appl. Phys.* **28**, L1959 (1989).
- ⁴³D. Jayne, *J. Vac. Sci. Technol. A* **8**, 147 (1990).
- ⁴⁴A. Savitzky and M. J. E. Golay, *Anal. Chem.* **36**, 1627 (1964).
- ⁴⁵D. A. Shirley, *Phys. Rev. B* **5**, 4709 (1972).
- ⁴⁶K. Okada, J. Kawai, and A. Kotani, Technical Report of ISSP, Ser. A, No. 2639 (1993).
- ⁴⁷T. Åberg, *Phys. Rev.* **156**, 35 (1967).
- ⁴⁸J. Kawai, C. Satoko, K. Fujisawa, and Y. Gohshi, *Phys. Rev. Lett.* **57**, 988 (1986).
- ⁴⁹J. Kawai, K. Nakajima, and Y. Gohshi, *Spectrochim. Acta B* (to be published).
- ⁵⁰G. B. Armen, T. Åberg, K. R. Karim, J. C. Levin, B. Crasemann, G. S. Brown, M. H. Chen, and G. E. Ice, *Phys. Rev. Lett.* **54**, 182 (1985).
- ⁵¹L. Landau, *Physik. Z. Sowjetunion* **1**, 88; **2**, 46 (1932).
- ⁵²C. Zener, *Proc. R. Soc. London Ser. A* **137**, 696 (1933); **140**, 660 (1933).
- ⁵³H. Eyring, J. Walter, and G. E. Kinball, *Quantum Chemistry* (Wiley, New York, 1944), pp. 326-330.
- ⁵⁴P. R. Wood and D. S. Urch, *Chem. Phys. Lett.* **37**, 13 (1976).
- ⁵⁵C. F. Hague, J.-M. Mariot, and H. Ostrowiecki, in *Proceedings of the International Conference on X-Ray and XUV Spectroscopy*, Sendai, 1978 [*Jpn. J. Appl. Phys.* **17**, 105 (1978)].
- ⁵⁶I. R. Holton, P. Weightman, and P. T. Andrews, *J. Phys. C* **16**, 3607 (1983).